Multivalent Cluster Nanomolecules for Inhibiting Protein-Protein Interactions

Elaine A. Qian,[1,2,3] Yanxiao Han,[4] Marco S. Messina,[1,3] Heather D. Maynard,[1,2,3] Petr Král,[4,5,6] and Alexander M. Spokoyny[1,3]*

[1]Department of Chemistry and Biochemistry, [2]Department of Bioengineering, and [3]California NanoSystems Institute, University of California, Los Angeles, California 90095, United States

[4]Department of Chemistry, [5]Department of Physics, and [6]Department of Biopharmaceutical Sciences, University of Illinois at Chicago, Chicago, Illinois 60607, United States

*E-mail: spokoyny@chem.ucla.edu

Abstract

Multivalent protein-protein interactions serve central roles in many essential biological processes, ranging from cell signaling and adhesion to pathogen recognition. Uncovering the rules that govern these intricate interactions is important not only to basic biology and chemistry, but also to the applied sciences where researchers are interested in developing molecules to promote or inhibit these interactions. Here we report the synthesis and application of atomically precise inorganic cluster nanomolecules consisting of an inorganic core and a covalently linked densely-packed layer of saccharides. These hybrid agents are stable under biologically relevant conditions and exhibit multivalent binding capabilities, which enable us to study the complex interactions between glycosylated structures and a dendritic cell lectin receptor. Importantly, we find that subtle changes in the molecular structure lead to significant differences in the nanomolecule's protein-binding properties. Furthermore, we demonstrate an example of using these hybrid nanomolecules to effectively inhibit protein-protein interactions in a human cell line. Ultimately, this work reveals an intricate interplay between the structural design of multivalent agents and their biological activities toward protein surfaces.

24 Multivalency is a prevalent phenomenon that facilitates many important biological processes in
25 nature.[1] Some of the most fascinating examples are found in our own immune system, where
26 multivalency plays a crucial role in modulating several central functions of the immune cells,
27 including cell signaling, cell-cell interaction, and pathogen recognition.[2–5] A notable example of
28 these intricate interactions takes place between glycoproteins and lectins, whose specificity and
29 affinity toward each other are greatly amplified through multivalency. The important role
30 multivalency plays in nature has fascinated both biologists and chemists alike, who are mutually
31 interested in understanding the fundamental mechanisms behind these supramolecular recognition
32 events as well as developing abiotic tools that are inspired by natural phenomena.[5–9]
33 An important biological target for studying multivalency is a C-type lectin receptor called
34 dendritic cell-specific intercellular adhesion molecule-3-grabbing nonintegrin (DC-SIGN).[10]
35 Predominately expressed on the surface of dendritic cells, it organizes into a homotetrameric
36 structure that is critical for the multivalent recognition of pathogens.[11,12] In particular, DC-SIGN
37 is able to bind specific high-mannose glycoproteins and glycolipids on pathogens with high
38 avidity, which activates a sequence of downstream responses including pathogen uptake and
39 degradation as well as subsequent antigen processing and presentation.[13] However, various
40 pathogens such as HIV-1 have been observed to escape the intracellular degradation pathway
41 following DC-SIGN-facilitated uptake.[14] While the mechanism behind this unusual behavior is
42 not well understood, it is clear that DC-SIGN plays an instrumental role in transmitting HIV-1 to
43 the T cells and enhancing the infection in its early stages.[14–16] Therefore, there is significant interest
44 in 1) uncovering the rules that govern the multivalent interactions between DC-SIGN and high-
45 mannose glycoconjugates and 2) inhibiting the DC-SIGN-dependent attachment and uptake of
46 certain pathogens. One of the most promising approaches that can potentially tackle both

47 challenges is centered around building molecules that can mimic the dense multivalent display of
48 carbohydrates on the pathogen surface.[8,9,17–19]

49 Previously, several promising classes of glycomimetic ligands for DC-SIGN have been
50 designed and synthesized, which include but are not limited to small molecules,[20,21] peptides,[22,23]
51 linear and dendritic polymers,[24–30] fullerenes,[31,32] supramolecular assemblies,[33–35] and hybrid
52 nanoparticles.[36–38] These constructs are capable of engaging DC-SIGN with high avidities (K_D
53 spanning nM–μM), which allowed several of these systems to inhibit viral entry and infection. In
54 particular, rigid three-dimensional (3D) architectures such as thiol-capped gold nanoparticles
55 (AuNPs) are attractive glycomimetic platforms due to the ease of generating tunable and well-
56 defined multivalent agents. Nevertheless, due to the weak bonding interactions between gold and
57 thiol-based ligands, the surface morphology of these systems is poorly defined and highly
58 dynamic, especially under biologically relevant conditions.[39–42] This ultimately hinders
59 researchers' ability to understand the precise structure-activity relationships of these systems with
60 respect to biomolecular recognition and binding events.

61 Here we report the synthesis of a family of atomically precise glycosylated cluster
62 nanomolecules featuring robust inorganic cluster scaffolds as nanoparticle core templates.
63 Specifically, we developed conditions that allow the rapid functionalization of perfluoroaryl-based
64 moieties covalently grafted onto a rigid dodecaborate core *via* "click"-like nucleophilic aromatic
65 substitution (S_NAr) chemistry, thus leading to fully covalent nanomolecules with a densely packed
66 layer of saccharides.[43,44] This chemistry mimics the operational simplicity with which thiol-capped
67 AuNPs are synthesized, yet produces well-defined assemblies that are stable under biologically
68 relevant conditions.[44] Importantly, direct binding studies between these hybrid assemblies and DC-
69 SIGN reveal the multivalency-enhanced avidity in addition to the carbohydrate specificity of the

70 lectin and the structural requirements for the multivalent ligands. Furthermore, competitive
71 binding data suggest the mannose-coated nanomolecules can inhibit the protein-protein
72 interactions between DC-SIGN and an HIV-1 envelope glycoprotein, gp120. Moreover, we found
73 that the nanomolecules exhibit no apparent toxicity to a human lymphoblast-like cell line at 0.5–
74 50 μM concentrations. This allowed us to perform cellular experiments, which revealed that the
75 mannose-functionalized clusters are capable of preventing the cell uptake of gp120 by blocking
76 cell-surface DC-SIGN. Therefore, we demonstrate that easily accessible, precisely engineered
77 hybrid cluster-based nanomolecules can be utilized to not only study the rules governing
78 multivalent recognition, but also inhibit protein-protein interactions in cells.

79 **Results and Discussion**

80 Given our success in installing a wide scope of thiols onto the perfluoroaryl-perfunctionalized
81 clusters using S_NAr chemistry,[44] we hypothesized that this strategy could be applied to generate a
82 library of atomically precise nanomolecules featuring a variety of saccharides densely packed on
83 the rigid 3D surface. Using the perfluoroaryl-perfunctionalized cluster **2** (Figure 1a) and 1-thio-*β*-
84 D-mannose tetraacetate,[44–47] we performed S_NAr reactions in the presence of base in
85 dimethylformamide (DMF), stirring under a N_2 atmosphere. These test conjugation reactions
86 revealed significant conversions, as determined by ^{19}F NMR spectroscopy. Following efficient
87 optimization facilitated by *in situ* ^{19}F NMR spectroscopy, we found that employing an excess of
88 the thiol and potassium phosphate (K_3PO_4) allowed the nearly quantitative (≥99%) substitution of
89 **2** with the substrate within 48 hours. The product was briefly treated with sodium methoxide
90 (NaOMe) to remove all the acetyl groups, then purified by a desalting centrifugal filter to yield the
91 mannose-coated nanomolecule **2a** (Table 1, entry 1) in 80% isolated yield (see the Supporting
92 Information for experimental details). The purified **2a** was subsequently subjected to

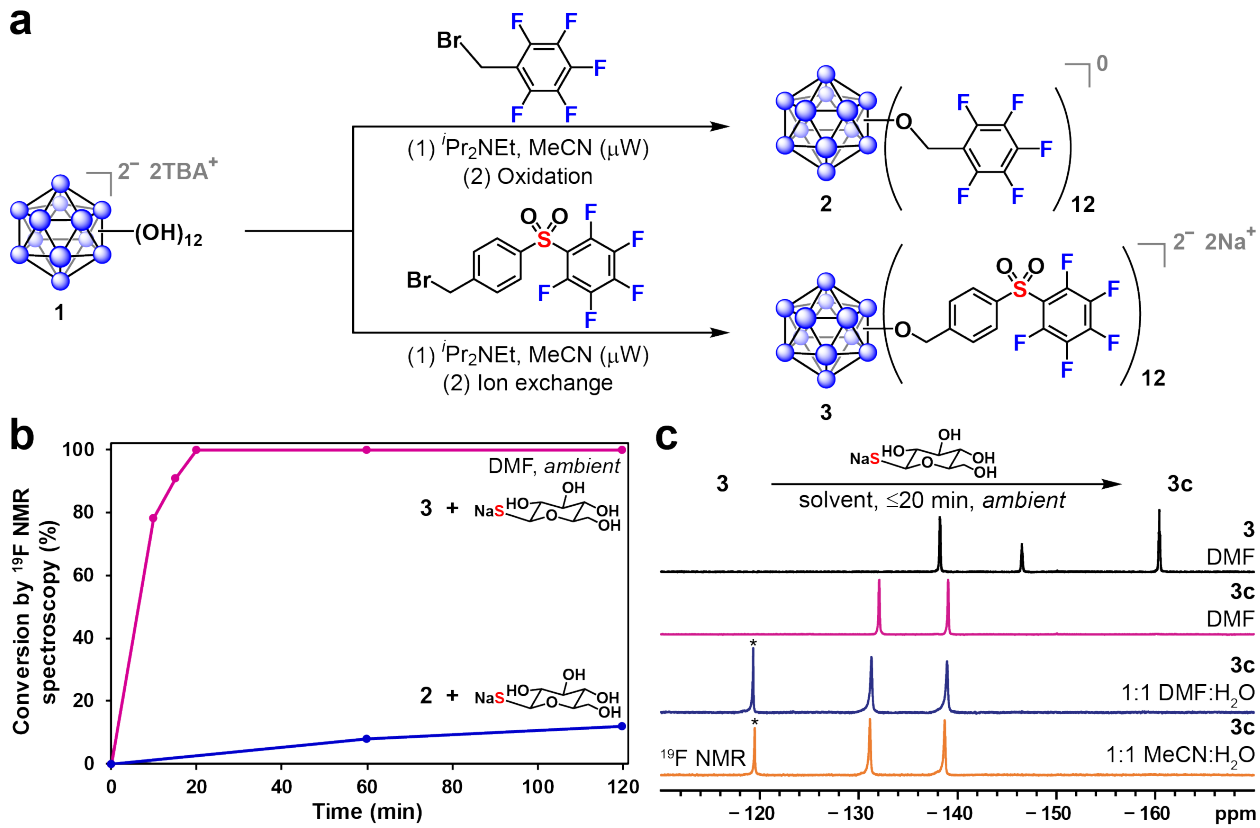

Figure 1. Synthesis of perfluoroaryl-perfunctionalized clusters and their reactivities toward an unprotected thiolated saccharide. (a) Clusters **2** and **3** are readily prepared from **1** with the assistance of a microwave reactor. (b) Conversion rates of S_NAr reactions between **2**/**3** and 1-thio-*β*-D-glucose sodium salt, as monitored by ^{19}F NMR spectroscopy, reveal the significantly enhanced reactivity of **3** over **2**. (c) ^{19}F NMR spectra of **3** in DMF and **3c** after conjugation with 1-thio-*β*-D-glucose sodium salt in DMF or mixed aqueous/organic media. *NaF signal.

characterization *via* ^{1}H, ^{11}B, and ^{19}F NMR spectroscopy and electrospray ionization-high resolution mass spectrometry (ESI-HRMS), which support the proposed structure and composition (see the Supporting Information for characterization data). Furthermore, we found that a similar strategy could be used to perfunctionalize **2** with 1-thio-*β*-D-galactose tetraacetate within 48 hours,[47,48] giving rise to the purified nanomolecule **2b** (Table 1, entry 2), after isolation in 84% yield (see the Supporting Information for experimental details and characterization data). Additionally, we prepared previously reported glucose- and poly(ethylene glycol) (PEG)-coated structures **2c** and **2d** (Table 1, entries 3 and 4),[44] and notably the isolated yield for **2c** was

Table 1. Glycosylation and PEGylation of Clusters 2 and 3

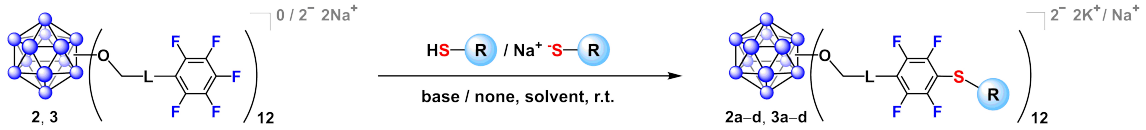

Entry	Compound	L	R	Time (h)	*In situ* yield[a] (%)	Isolated yield[b] (%)
1	**2a**	none	mannose	48	≥99	80
2	**2b**	none	galactose	48	≥99	84
3	**2c***	none	glucose	24	≥99	65
4	**2d***	none		24	≥99	76
5	**3a**		mannose	0.3	≥99	83
6	**3b**		galactose	0.3	≥99	67
7	**3c**		glucose	0.3	≥99	77
8	**3d**			1.5	≥99	84

[a]Yield determined by ^{19}F NMR spectroscopy; [b]Isolated yield after purification; *Previously reported compounds. r.t., room temperature.

significantly improved (17% to 65%) through the new purification strategy (see the Supporting Information for experimental details). Overall, these results demonstrate that perfluoroaryl-thiol S_NAr chemistry can be utilized to assemble a panel of well-defined, multivalent hybrid nanomolecules functionalized with various saccharides including mannose, galactose, and glucose. Moreover, both the glycosylated and PEGylated nanomolecules can be easily purified using desalting centrifugal filters, which streamlines access to the pure materials. Ultimately, these nanomolecules provide us with the ability to evaluate the biological activities of multivalent assemblies as a function of the molecular structure precisely displayed in 3D space.

With the successful synthesis of glycosylated nanomolecules **2a**–**c**, we sought to build a new generation of multivalent architectures that share the precision and rigidity of the first-generation assemblies, but feature a rationally designed linker that will modularly extend the cluster scaffold. We envisioned that the new class of larger-sized glycosylated nanomolecules featuring a distinct multivalent display of saccharides, when studied alongside **2a**–**c**, will allow us to further investigate the complex relationship between molecular structure and activity in the multivalent constructs. Keeping the downstream biological applications in mind, we set out to find a rigid linker that could ideally lead to water-soluble glycosylated nanomolecules. After testing multiple linker designs, we found a sulfone-bridged biphenyl derivative (Figure 1a) to be the most suitable candidate. The rationale behind choosing this linker was two-fold – not only could the polar sulfone group promote the overall water solubility of the nanomolecule (our attempt to use a biphenyl motif resulted in a poorly water-soluble glycosylated cluster), but also a similar molecule, decafluoro-biphenylsulfone, was recently found to exhibit remarkably fast S_NAr reactivity toward cysteine residues on peptides under aqueous conditions.[49] Therefore, we hypothesized that perfunctionalization of **1** (Figure 1a) with the sulfone-bridged linker could enhance the S_NAr reaction kinetics and impart aqueous compatibility to the cluster conjugation, resulting in a water-soluble glycosylated species. The target benzyl bromide linker containing a terminal $SO_2C_6F_5$ functional group was synthesized in three steps (see the Supporting Information for experimental details and characterization data). Using a microwave-assisted synthesis method,[50] we observed nearly quantitative conversion of **1** to the perfunctionalized cluster within 30 minutes, based on ^{11}B NMR spectroscopy and ESI-HRMS. The cluster species was isolated from the residual organic-based starting materials *via* silica gel chromatography in 94% yield. After subjecting the compound to a sodium ion exchange column, **3** (Figure 1a) was isolated as a light salmon-colored

solid (see the Supporting Information for experimental details). ^{1}H, ^{11}B, and ^{19}F NMR spectroscopy (Figure 1c) and ESI-HRMS results of **3** are consistent with the proposed structure and composition of the dodeca-functionalized B_{12}-based cluster (see the Supporting Information for characterization data).

To test whether cluster **3** exhibits enhanced S_NAr reactivity toward thiols, we exposed **3** dissolved in DMF to a stoichiometric amount of an unprotected thiolated saccharide, 1-thio-*β*-D-glucose sodium salt, and observed by ^{19}F NMR spectroscopy a nearly quantitative (≥99%) conversion to **3c** (Table 1, entry 7) within 20 minutes (Figure 1b, c). The purified water-soluble **3c** was obtained *via* a desalting centrifugal filter, and was subjected to analysis *via* ^{1}H, ^{11}B, and ^{19}F NMR spectroscopy and ESI-HRMS, which support the proposed structure and composition (see the Supporting Information for experimental details and characterization data). Notably, due to the rapid kinetics, this reaction did not require a N_2 atmosphere in order to proceed to completion, therefore all subsequent conjugation reactions of **3** were performed under ambient conditions. Parallel experiments monitoring the S_NAr reaction conversion over time of **2** and **3** by ^{19}F NMR spectroscopy revealed the significantly improved conversion rates of **3** over **2** (Figure 1b), which is consistent with our hypothesis. We then proceeded to test whether **3** tolerates water in the conjugation reaction by subjecting **3** to a stoichiometric amount of 1-thio-*β*-D-glucose sodium salt in 1:1 DMF:water and 1:1 acetonitrile (MeCN):water mixtures, and in both cases observed nearly quantitative (≥99%) conversion to **3c** within 15 minutes (Figure 1c) (see the Supporting Information for experimental details). These remarkably fast reaction kinetics in mixed aqueous/organic media are consistent with the observations by Kalhor-Monfared *et al.* and furthermore may be facilitated by the enhanced solubility of 1-thio-*β*-D-glucose sodium salt in water.[49] Overall, these studies demonstrate that by employing rational linker design, the S_NAr

155 reaction characteristics including kinetics and aqueous compatibility can be dramatically
156 enhanced, allowing for the rapid assembly of atomically precise, densely glycosylated
157 nanomolecules.

158 Based on the successful glycosylation of **2** to yield functionalized nanomolecules **2a**–**c**, we
159 hypothesized that **3** could likewise be glycosylated by mannose and galactose in addition to
160 glucose (*vide supra*). Treatment of **3** with the sodium salts of 1-thio-*α*-D-mannose and 1-thio-*β*-
161 D-galactose in 1:1 DMF:water mixtures resulted in nearly quantitative (≥99%) conversions within
162 15 minutes to **3a** and **3b** (Table 1, entries 5 and 6), respectively. Following purification, **3a** and **3b**
163 were subjected to characterization *via* ^{1}H, ^{11}B, and ^{19}F NMR spectroscopy and ESI-HRMS, which
164 support the proposed structures and compositions (see the Supporting Information for
165 experimental details and characterization data). Furthermore, we were able to fully PEGylate **3**
166 within 90 minutes, giving rise to purified **3d** (Table 1, entry 8) after isolation in 84% yield (see the
167 Supporting Information for experimental details and characterization data). These experiments
168 demonstrate that cluster **3** can rapidly lead to a library of multivalent hybrid entities featuring
169 diverse functional groups, which allows us to study how the specific surface chemistry affects the
170 protein-binding properties. Ultimately, the family of precisely engineered multivalent
171 nanomolecules (**2a**–**3** and **3a**–**d**, *vide supra*) creates a framework which can potentially enable us
172 to study the fundamental rules that govern multivalent biological recognition events.

173 Following the assembly and isolation of the glycosylated and PEGylated clusters, we proceeded
174 to uncover the binding characteristics of the various nanomolecules toward an important dendritic
175 cell receptor, DC-SIGN. Among the existing techniques that can experimentally elucidate the
176 binding affinities between complex molecules and biomolecular targets, the surface plasmon
177 resonance (SPR) technology represents a "gold standard" used by researchers in both academic

178 and biotechnology communities.[51,52] Given the ability of the SPR technology to perform real-time,
179 label-free detection of biomolecular interactions with high sensitivity,[52] we decided to use it for
180 studying the binding interactions between the multivalent cluster nanomolecules and DC-SIGN.
181 In the first set of SPR-based direct binding experiments, the tetrameric DC-SIGN extracellular
182 domain (ECD) was immobilized on a commercial sensor chip *via* standard amide coupling, and
183 the mannose-functionalized nanomolecules **2a** and **3a** were injected over the protein surface for
184 real-time visualization of their respective binding interactions with DC-SIGN (see the Supporting
185 Information for experimental details). The resulting sensorgrams (Figure 2a, d) reflect changes in
186 the refractive index as molecules interact with the lectin surface, and reveal the dose-dependent
187 binding response of **2a** and **3a**, respectively, toward DC-SIGN. By fitting the Langmuir 1:1 binding
188 model to the binding curves of the mannose-coated clusters, we estimated K_D values of 0.11 μM
189 for **2a** and 5.0 μM for **3a**. Compared to D-mannose (low mM affinity),[11] these multivalent systems
190 exhibit avidities three to four orders of magnitude higher for DC-SIGN through the cluster
191 glycoside effect.[3] To further understand the dynamics of the multivalent interactions, we
192 performed computational studies using a tetrameric model derived from an X-ray structure of DC-
193 SIGN (see the Supporting Information for experimental details).[12,53] Molecular dynamics (MD)
194 simulations of the interactions between the DC-SIGN model and **2a**/**3a** over 40 ns were conducted,
195 and snapshots were taken at the end of both simulations (Figure 2b–c/e–f, respectively; see the
196 Supporting Information for experimental details and movies). The MD movies and snapshots
197 suggest that consistent with previous reports using monosaccharides and oligosaccharides,[11,12] the
198 equatorial 3-OH and 4-OH groups on the cluster-linked mannose residues engage in Ca^{2+}-mediated
199 binding in the carbohydrate recognition sites. Furthermore, **2a** was observed to stay longer than **3a**
200 near the binding site of the protein model (Figure S16), which agrees with the lower K_D value of

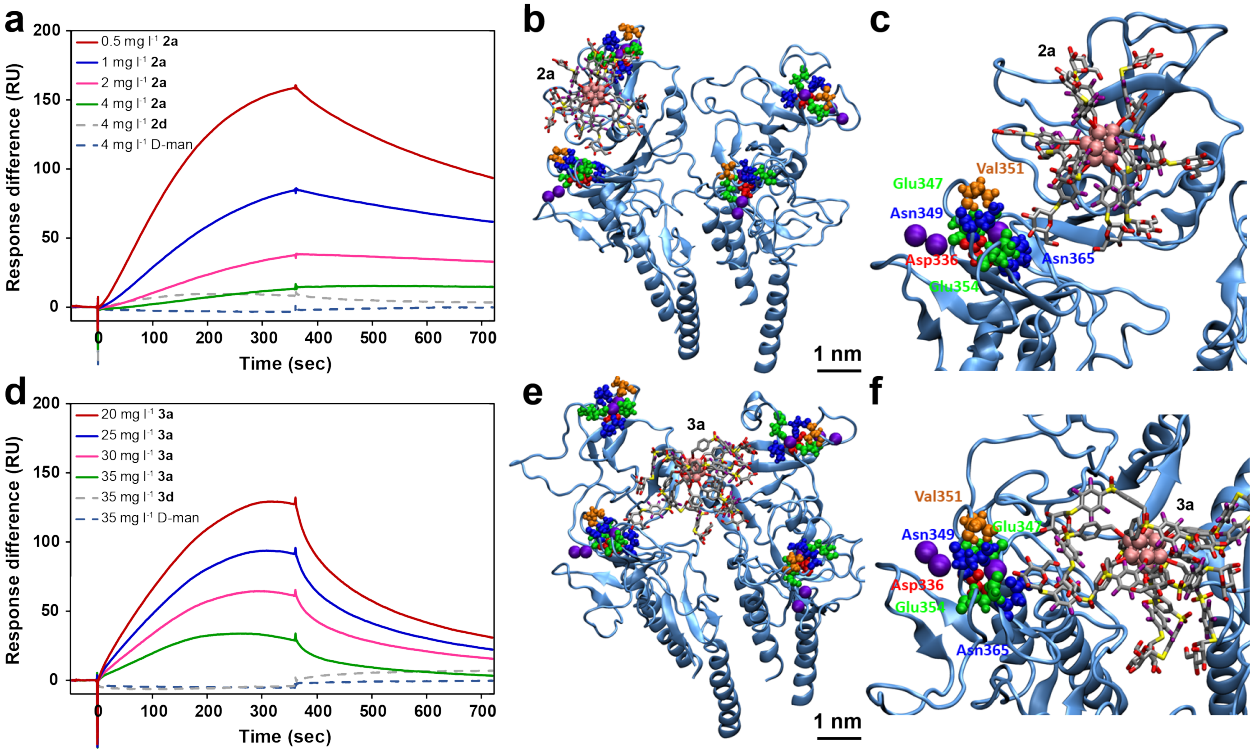

Figure 2. Multivalent binding interactions between mannose-functionalized nanomolecules and DC-SIGN. (a, d) SPR sensorgrams reveal dose-dependent multivalent binding of **2a** and **3a** to DC-SIGN, respectively, while the controls PEGylated clusters (**2d** and **3d**) and D-mannose exhibit minimal to no binding to DC-SIGN. In all SPR experiments, the flow rate is 5 μL/min, and the analytes are injected for 6 minutes, followed by buffer flow. (b, e) Snapshots after 40 ns of MD simulations of the binding interactions between **2a**/**3a** and DC-SIGN. (c, f) Zoomed-in snapshots reveal each nanomolecule binding to the carbohydrate recognition sites of DC-SIGN. See the Supporting Information for the MD simulation movies.

201 **2a** determined from the SPR experiments. A possible explanation for the observed difference in
202 avidity is the flexibility of the linker – while the extended linker in **3a** is still rigid, it allows more
203 flexibility compared to the benzylic linker in **2a**. Although a more flexible linker can relax the
204 requirements for the precise positioning of ligands on a multivalent scaffold, it can also lower the
205 overall affinity for a target protein.[5]

206 After analyzing the binding interactions of mannose-coated cluster nanomolecules toward DC-
207 SIGN, we hypothesized that the clusters grafted with other saccharides would exhibit different
208 protein-binding behaviors. Therefore, we conducted another set of SPR-based direct binding
209 studies with the glucose-coated nanomolecules (**2c** and **3c**) (Figures S1 and S2), which yielded K_D

210 values of 0.18 and 30 μM, respectively. These similar but slightly higher K_D values compared to
211 the mannose-coated analogs agree with results from previous reports using monosaccharides,[11,54]
212 which suggest the equatorial 3- and 4-OH groups on glucose allow a similar binding interaction
213 with DC-SIGN. In contrast, the galactose-coated species (**2b** and **3b**) were unable to engage DC-
214 SIGN with similar avidities (the estimated K_D values were 0.87 and 96 μM, respectively; Figures
215 S3 and S4). This finding is also consistent with prior reports with monosaccharides and
216 glycopolymers,[11,24,54] since the axial 4-OH group on galactose prevents proper recognition by the
217 carbohydrate-binding sites on DC-SIGN. In contrast, the controls – PEGylated clusters (**2d** and
218 **3d**) and D-mannose – exhibit minimal to no binding to the protein surface when injected at the
219 highest mass concentrations with respect to **2a** and **3a** (Figure 2a, d). Overall, these experiments
220 reveal the dramatically enhanced binding avidities of the glycosylated cluster nanomolecules as a
221 result of multivalency and highlight a potentially intricate relationship between the scaffold
222 flexibility and the binding affinity. Nevertheless, in nature DC-SIGN is known to be a very flexible
223 transmembrane receptor that can reposition its carbohydrate recognition domains to adapt to the
224 ligands,[55] and this dynamic behavior is not fully captured by the immobilized protein setup in the
225 *in vitro* SPR and *in silico* MD experiments.

226 Therefore, we turned to SPR-based competitive binding assays in order to test 1) whether free
227 (vs immobilized) DC-SIGN exhibits different binding characteristics to the cluster nanomolecules
228 and 2) whether the mannose-coated species can inhibit the protein-protein interactions between
229 DC-SIGN and a sub-nM binder, HIV-1 gp120.[24,56] In these competition experiments, 100 nM DC-
230 SIGN and various concentrations of the nanomolecules were co-injected over the surface-
231 immobilized gp120, and the binding response of each injection was compared to that of each
232 preceding injection of DC-SIGN alone for an estimation of the % inhibition of the DC-SIGN–

233 gp120 interaction. As shown in Figure 3, **2a**
234 and **3a** can both inhibit free DC-SIGN from
235 attaching to gp120, with IC_{50} values of 2.0 and
236 5.2 μM, respectively. These values are over
237 three orders of magnitude lower than the
238 reported IC_{50} of monovalent D-mannose (6–9
239 mM),[54,57] indicating dramatically enhanced
240 inhibition. Notably, compared with the IC_{50}
241 values from a similar SPR-based competition
242 assay using a multivalent third-generation
243 dendrimer (50 μM, 32 mannose residues),[27]
244 these values are an order of magnitude lower.
245 These results suggest that rigid inorganic
246 cluster-based nanomolecules featuring
247 significantly fewer (12) saccharides can serve
248 as more potent inhibitors of this protein-protein
249 interaction. Furthermore, in agreement with the

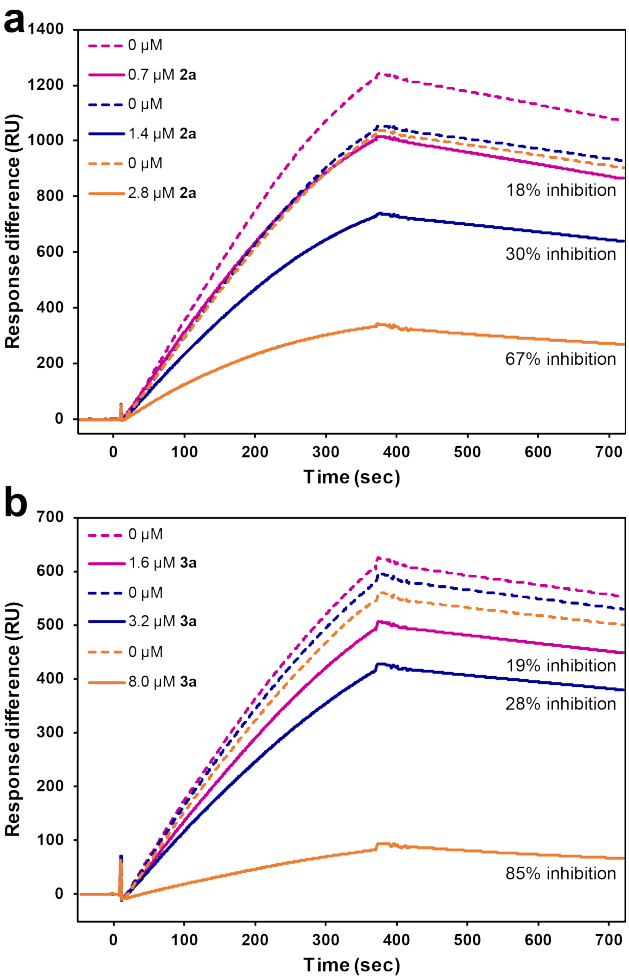

Figure 3. Mannose-functionalized clusters are capable of inhibiting protein-protein interactions. (a, b) SPR-based competitive binding studies suggest that **2a** and **3a** effectively compete against immobilized gp120 to bind free DC-SIGN, which leads to reduced binding responses.

250 direct binding data, the galactose-coated (**2b**, **3b**) and PEGylated (**2d**, **3d**) nanomolecules as well
251 as D-mannose were less successful at inhibiting this interaction (Figures S5 and S6). Overall, these
252 competition studies demonstrate for the first time the ability of multivalent glycosylated cluster
253 nanomolecules to effectively compete against a sub-nM-binding viral glycoprotein for DC-SIGN.
254 This suggests that a rigid cluster scaffold-based multivalent display of carbohydrates that mimics
255 the natural highly glycosylated proteins on the surface of pathogens can be engineered to inhibit

256 the interactions between a cell-based lectin receptor and a viral glycoprotein. Moreover, the
257 similarity in IC_{50} values for **2a** and **3a** in contrast to their different K_D values could be due to a
258 combination of the free (vs immobilized) DC-SIGN better adapting to the more flexible
259 nanomolecule **3a** and the greater receptor surface coverage by the larger nanomolecule **3a**.

260 To further investigate the ability of the mannose-functionalized cluster nanomolecules to inhibit
261 the protein-protein interactions between DC-SIGN and gp120 in an experimental setup more
262 reminiscent of natural systems, we moved to cell-based studies using a DC-SIGN-expressing
263 human lymphoblast-like cell line (Raji DC-SIGN+ cells) and HIV-1 gp120 (Figure 4a).[58,59] First,
264 in order to gain a better understanding of the biocompatibility of the cluster nanomolecules, we
265 conducted an MTS-based cell proliferation assay (see the Supporting Information for experimental
266 details), and observed no apparent cytotoxic effects of the mannose-coated (**2a**, **3a**) and PEGylated
267 (**2d**, **3d**) clusters toward Raji DC-SIGN+ cells at 0.5–50 μM concentrations (Figure 4b). This
268 finding allowed the evaluation of the nanomolecules' potential biological function in inhibiting
269 the attachment of gp120 to cell-surface DC-SIGN. Fluorescein isothiocyanate-labeled gp120
270 (gp120-FITC) undergoes significant uptake by Raji DC-SIGN+ cells (Figure 4c), as observed by
271 a confocal laser scanning microscopy-based assay (see the Supporting Information for
272 experimental details and Figures S7–S15). This internalization is DC-SIGN-dependent since no
273 gp120-FITC uptake was observed in a Raji cell line not expressing DC-SIGN (Figure 4c).[60,61] In
274 order to test competitive inhibition, we introduced mixtures of gp120-FITC and mannose-coated
275 clusters **2a**/**3a** to Raji DC-SIGN+ cells, and observed reduced gp120-FITC uptake as a function of
276 the cluster concentration (10 to 25 μM) (Figure 4c). Notably, at the same concentrations, **3a** was
277 more effective than **2a** at preventing the binding and uptake of gp120-FITC. This result suggests
278 that **3a** can bind DC-SIGN in its natural transmembrane conformation better, which could be due

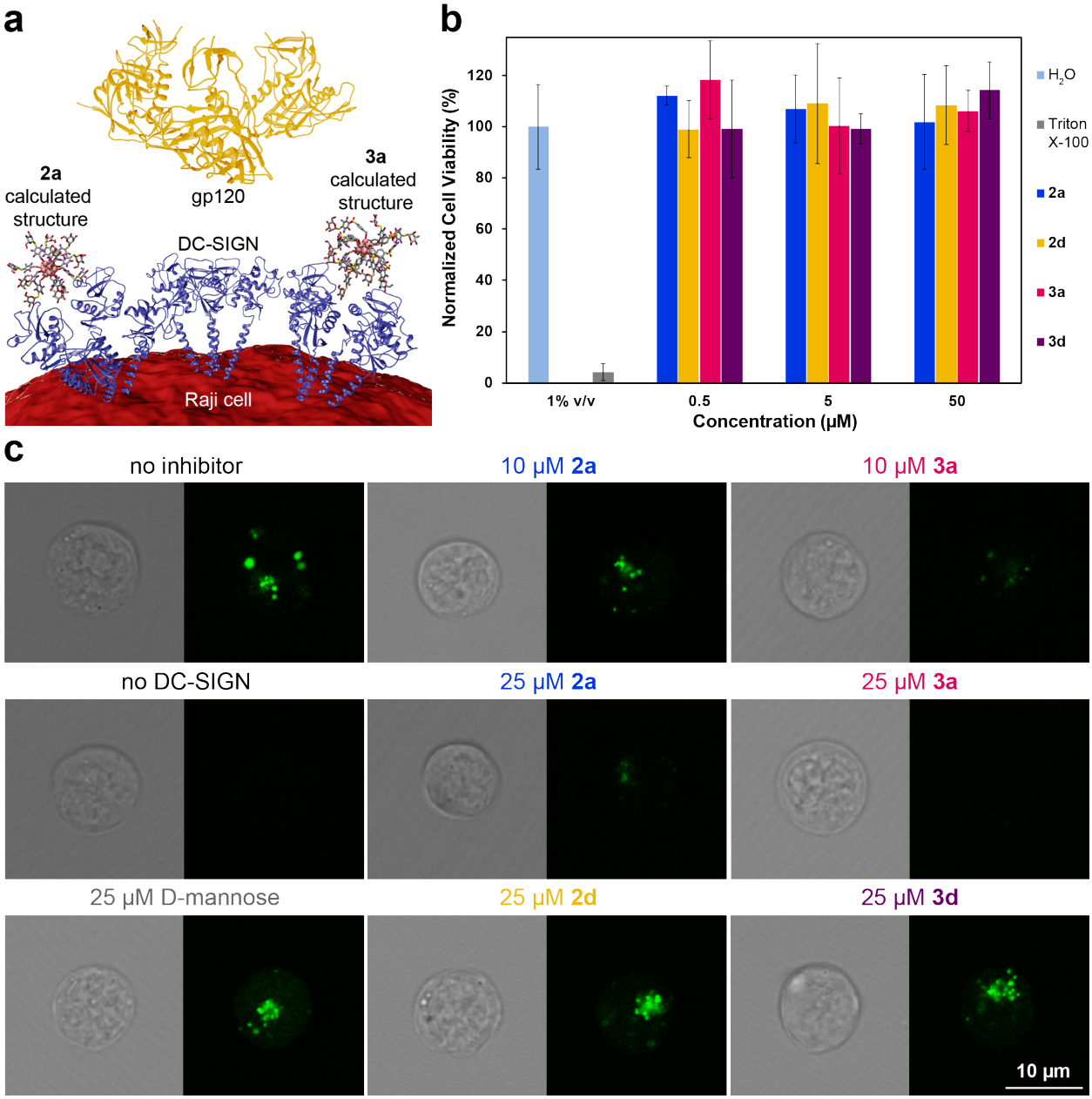

Figure 4. Biocompatible mannose-coated cluster nanomolecules can serve as multivalent inhibitors to prevent the DC-SIGN-mediated cell uptake of gp120. (a) Glycosylated clusters can potentially inhibit the uptake of viral glycoproteins such as gp120 by blocking cell-surface DC-SIGN. Figure is not drawn to scale. (b) Mannose-coated and PEGylated clusters exhibit no apparent toxicity toward Raji DC-SIGN+ cells at least up to 50 μM, as assessed by an MTS assay. (c) DC-SIGN-dependent cell uptake of gp120-FITC is inhibited by mannose-coated clusters (**2a** and **3a**), as indicated by confocal microscopy analysis. However, the controls PEGylated clusters (**2d** and **3d**) and D-mannose do not affect the uptake of gp120-FITC.

279 to its higher flexibility and larger size. Furthermore, these cell-based studies capture important

280 information about the dynamic receptor-mediated antigen internalization process,[62] thus enabling

281 us to assess both the nanomolecules' binding to DC-SIGN and the inhibition of antigen uptake.
282 Consistent with the presented SPR-based direct and competitive binding data, the control
283 molecules – PEGylated clusters (**2d** and **3d**) and D-mannose – were not able to bind to DC-SIGN
284 and inhibit gp120 uptake at 25 μM (Figure 4c). Overall, the biological studies in cells reveal that
285 biocompatible mannose-functionalized cluster nanomolecules are capable of competing against
286 HIV-1 gp120 for cell-surface DC-SIGN and thereby preventing the receptor-mediated
287 internalization of a viral envelope component.

288 **Conclusions**

289 We have demonstrated the rapid assembly of multivalent glycosylated inorganic cluster
290 nanomolecules capable of inhibiting protein-protein interactions. Specifically, a dense layer of
291 thiolated saccharides can be grafted on a rigid perfluoroaryl-perfunctionalized B_{12} cluster within
292 15 minutes in mixed aqueous/organic media using S_NAr chemistry. The resulting fully covalent
293 glycosylated assemblies can serve as multivalent binders with dramatically enhanced affinity
294 compared to monovalent saccharides toward target lectins. We showed an example of using these
295 hybrid agents for engendering ligand-specific, multivalent recognition with a biologically
296 important dendritic cell receptor, DC-SIGN. Importantly, we demonstrated the ability of the cluster
297 nanomolecules to inhibit protein-protein interactions between DC-SIGN and a sub-nM-binding
298 HIV-1 envelope glycoprotein in a competitive binding study. We further found these clusters to
299 be biocompatible in a human cell line and capable of preventing the internalization of gp120 by
300 DC-SIGN-expressing cells. Notably, we uncovered an intricate interplay between the structural
301 designs of multivalent binders and their biological activities. Ultimately, this work showcases a
302 rare example of the application of tunable, stable inorganic cluster-based nanomolecules as

303 valuable tools for studying the rules that govern multivalent interactions and disrupting protein-
304 protein interactions.[63–65]

305 **Safety Statement**

306 No unexpected or unusually high safety hazards were encountered.

307 **Supporting Information**

308 The Supporting Information is available free of charge on the ACS Publications website.

309 All methods, synthetic procedures, characterization data, supplementary data, and MD
310 simulation movies.

311 **Corresponding Author**

312 *E-mail: spokoyny@chem.ucla.edu

313 **ORCID**

314 Elaine A. Qian: 0000-0002-7111-7383

315 Marco S. Messina: 0000-0003-2827-118X

316 Heather D. Maynard: 0000-0003-3692-6289

317 Petr Král: 0000-0003-2992-9027

318 Alexander M. Spokoyny: 0000-0002-5683-6240

319 **Author Contributions**

320 E.A.Q. and A.M.S. conceived the project and composed the manuscript. E.A.Q. designed and
321 performed the experiments and analyzed the data. Y.H. and P.K. designed, conducted, and
322 interpreted the computational studies. M.S.M. and H.D.M. contributed to the synthesis of **2a** and
323 **2b**. All of the authors commented on the manuscript.

324 **Notes**

325 The authors declare no competing financial interest.

326 **Acknowledgments**

327 E.A.Q. thanks the NIH for the Predoctoral Training Fellowship through the UCLA Chemistry-
328 Biology Interface Training Program under the National Research Service Award (T32GM008496)
329 and the UCLA Graduate Division for the Dissertation Year Fellowship. M.S.M. is grateful to the
330 National Science Foundation (NSF) for the Bridge-to-Doctorate (HRD-1400789) and the
331 Predoctoral (DGE-0707424) Fellowships and UCLA for the Christopher S. Foote Fellowship.
332 H.D.M. thanks the Dr. Myung Ki Hong Endowed Chair in Polymer Science. A.M.S. thanks the
333 UCLA Department of Chemistry and Biochemistry for start-up funds, 3M for a Non-Tenured
334 Faculty Award, the Alfred P. Sloan Foundation for a Fellowship in Chemistry, Research
335 Corporation for Science Advancement (RCSA) for a Cottrell Scholar Award, and the National
336 Institutes of Health (NIH) for a Maximizing Investigators Research Award (MIRA,
337 R35GM124746). We are grateful for the assistance from Dr. Alex I. Wixtrom in optimizing the
338 synthesis of **2**. We thank UCLA Molecular Instrumentation Center for mass spectrometry (NIH
339 1S10OD016387-01) and NMR spectroscopy. We also thank the UCLA Biochemistry
340 Instrumentation Facility for use of the SPR instrument. The following reagents were obtained
341 through the NIH AIDS Reagent Program, Division of AIDS, NIAID, NIH: pcDNA3-DC-SIGN
342 from Drs. S. Pöhlmann, F. Baribaud, F. Kirchhoff, and R.W. Doms,[66] HIV-1 CM235 gp120
343 recombinant protein from NIAID, DAIDS, and both Raji and Raji DC-SIGN+ cells from Drs. Li
344 Wu and Vineet N. KewalRamani.[58]

345 **References**

346 (1) Mammen, M.; Choi, S.-K.; Whitesides, G. M. Polyvalent interactions in biological systems:
347 implications for design and use of multivalent ligands and inhibitors. *Angew. Chem., Int.*
348 *Ed.* **1998**, *37*, 2754–2794.

349 (2) Weis, W. I.; Taylor, M. E.; Drickamer, K. The C-type lectin superfamily in the immune
350 system. *Immunol. Rev.* **1998**, *163*, 19–34.

351 (3) Lundquist, J. J.; Toone, E. J. The cluster glycoside effect. *Chem. Rev.* **2002**, *102*, 555–578.

352 (4) Wolfert, M. A.; Boons, G. J. Adaptive immune activation: Glycosylation does matter. *Nat.*
353 *Chem. Biol.* **2013**, *9*, 776–784.

354 (5) *Multivalency*, 1st ed.; Huskens, J., Prins, L. J., Haag, R., Ravoo, B. J., Eds.; John Wiley &
355 Sons: Hoboken, NJ, 2018.

356 (6) Conn, M. M.; Rebek, J. Self-assembling capsules. *Chem. Rev.* **1997**, *97*, 1647–1668.

357 (7) Müller, C.; Despras, G.; Lindhorst, T. K. Organizing multivalency in carbohydrate
358 recognition. *Chem. Soc. Rev.* **2016**, *45*, 3275–3302.

359 (8) Bernardi, A.; Jiménez-Barbero, J.; Casnati, A.; De Castro, C.; Darbre, T.; Fieschi, F.; Finne,
360 J.; Funken, H.; Jaeger, K.-E.; Lahmann, M.; Lindhorst, T. K.; Marradi, M.; Messner, P.;
361 Molinaro, A.; Murphy, P. V.; Nativi, C.; Oscarson, S.; Penadés, S.; Peri, F.; et al.
362 Multivalent glycoconjugates as anti-pathogenic agents. *Chem. Soc. Rev.* **2013**, *42*, 4709–
363 4727.

364 (9) Bhatia, S.; Camacho, L. C.; Haag, R. Pathogen inhibition by multivalent ligand
365 architectures. *J. Am. Chem. Soc.* **2016**, *138*, 8654–8666.

366 (10) Geijtenbeek, T. B. H.; Torensma, R.; Vliet, S. J. Van; Duijnhoven, G. C. F. Van; Adema,
367 G. J.; Kooyk, Y. Van; Figdor, C. G. Identification of DC-SIGN, a novel dendritic cell-

368 specific ICAM-3 receptor that supports primary immune responses. *Cell* **2000**, *100*, 575–
369 585.
370 (11) Mitchell, D. A.; Fadden, A. J.; Drickamer, K. A novel mechanism of carbohydrate
371 recognition by the C-type lectins DC-SIGN and DC-SIGNR. Subunit organization and
372 binding to multivalent ligands. *J. Biol. Chem.* **2001**, *276*, 28939–28945.
373 (12) Feinberg, H.; Mitchell, D. a; Drickamer, K.; Weis, W. I. Structural basis for selective
374 recognition of oligosaccharides by DC-SIGN and DC-SIGNR. *Science* **2001**, *294*, 2163–
375 2166.
376 (13) Švajger, U.; Anderluh, M.; Jeras, M.; Obermajer, N. C-type lectin DC-SIGN: An adhesion,
377 signalling and antigen-uptake molecule that guides dendritic cells in immunity. *Cell. Signal.*
378 **2010**, *22*, 1397–1405.
379 (14) van Kooyk, Y.; Geijtenbeek, T. B. H. DC-SIGN: Escape mechanism for pathogens. *Nat.*
380 *Rev. Immunol.* **2003**, *3*, 697–709.
381 (15) Geijtenbeek, T. B. H.; Kwon, D. S.; Torensma, R.; Van Vliet, S. J.; Van Duijnhoven, G. C.
382 F.; Middel, J.; Cornelissen, I. L. M. H. A.; Nottet, H. S. L. M.; KewalRamani, V. N.;
383 Littman, D. R.; Figdor, C. G.; Van Kooyk, Y. DC-SIGN, a dendritic cell-specific HIV-1-
384 binding protein that enhances trans-infection of T cells. *Cell* **2000**, *100*, 587–597.
385 (16) Chung, N. P. Y.; Breun, S. K. J.; Bashirova, A.; Baumann, J. G.; Martin, T. D.;
386 Karamchandani, J. M.; Rausch, J. W.; Le Grice, S. F. J.; Wu, L.; Carrington, M.;
387 KewalRamani, V. N. HIV-1 transmission by dendritic cell-specific ICAM-3-grabbing
388 nonintegrin (DC-SIGN) is regulated by determinants in the carbohydrate recognition
389 domain that are absent in liver/lymph node-sign (L-SIGN). *J. Biol. Chem.* **2010**, *285*, 2100–
390 2112.

391 (17) Lepenies, B.; Lee, J.; Sonkaria, S. Targeting C-type lectin receptors with multivalent
392 carbohydrate ligands. *Adv. Drug Delivery Rev.* **2013**, *65*, 1271–1281.
393 (18) Kamiya, N.; Tominaga, M.; Sato, S.; Fujita, M. Saccharide-coated M12L24 molecular
394 spheres that form aggregates by multi-interaction with proteins. *J. Am. Chem. Soc.* **2007**,
395 *129*, 3816–3817.
396 (19) Zhang, Q.; Savagatrup, S.; Kaplonek, P.; Seeberger, P. H.; Swager, T. M. Janus emulsions
397 for the detection of bacteria. *ACS Cent. Sci.* **2017**, *3*, 309–313.
398 (20) Sattin, S.; Daghetti, A.; Thépaut, M.; Berzi, A.; Sánchez-Navarro, M.; Tabarani, G.; Rojo,
399 J.; Fieschi, F.; Clerici, M.; Bernardi, A. Inhibition of DC-SIGN-mediated HIV infection by
400 a linear trimannoside mimic in a tetravalent presentation. *ACS Chem. Biol.* **2010**, *5*, 301–
401 312.
402 (21) Borrok, M. J.; Kiessling, L. L. Non-carbohydrate inhibitors of the lectin DC-SIGN. *J. Am.*
403 *Chem. Soc.* **2007**, *129*, 12780–12785.
404 (22) Frison, N.; Taylor, M. E.; Soilleux, E.; Bousser, M.-T.; Mayer, R.; Monsigny, M.;
405 Drickamer, K.; Roche, A.-C. Oligolysine-based oligosaccharide clusters. *J. Biol. Chem.*
406 **2003**, *278*, 23922–23929.
407 (23) Ng, S.; Bennett, N. J.; Schulze, J.; Gao, N.; Rademacher, C.; Derda, R. Genetically-encoded
408 fragment-based discovery of glycopeptide ligands for DC-SIGN. *Bioorg. Med. Chem.* **2018**,
409 *26*, 5368–5377.
410 (24) Becer, C. R.; Gibson, M. I.; Geng, J.; Ilyas, R.; Wallis, R.; Mitchell, D. A.; Haddleton, D.
411 M. High-affinity glycopolymer binding to human DC-SIGN and disruption of DC-SIGN
412 interactions with HIV envelope glycoprotein. *J. Am. Chem. Soc.* **2010**, *132*, 15130–15132.
413 (25) Turnbull, W. B.; Stoddart, J. F. Design and synthesis of glycodendrimers. *Rev. Mol.*

414 *Biotechnol.* **2002**, *90*, 231–255.

415 (26) Lasala, F.; Arce, E.; Otero, J. R.; Rojo, J.; Delgado, R. Mannosyl glycodendritic structure
416 inhibits DC-SIGN-mediated Ebola virus infection in cis and in trans. *Antimicrob. Agents*
417 *Chemother.* **2003**, *47*, 3970–3972.

418 (27) Tabarani, G.; Reina, J. J.; Ebel, C.; Vivès, C.; Lortat-Jacob, H.; Rojo, J.; Fieschi, F.
419 Mannose hyperbranched dendritic polymers interact with clustered organization of DC-
420 SIGN and inhibit gp120 binding. *FEBS Lett.* **2006**, *580*, 2402–2408.

421 (28) Luczkowiak, J.; Sattin, S.; Sutkevičiute, I.; Reina, J. J.; Sánchez-Navarro, M.; Thépaut, M.;
422 Martínez-Prats, L.; Daghetti, A.; Fieschi, F.; Delgado, R.; Bernardi, A.; Rojo, J.
423 Pseudosaccharide functionalized dendrimers as potent inhibitors of DC-SIGN dependent
424 ebola pseudotyped viral infection. *Bioconjug. Chem.* **2011**, *22*, 1354–1365.

425 (29) Garcia-Vallejo, J. J.; Koning, N.; Ambrosini, M.; Kalay, H.; Vuist, I.; Sarrami-Forooshani,
426 R.; Geijtenbeek, T. B. H.; van Kooyk, Y. Glycodendrimers prevent HIV transmission via
427 DC-SIGN on dendritic cells. *Int. Immunol.* **2013**, *25*, 221–233.

428 (30) Ordanini, S.; Varga, N.; Porkolab, V.; Thépaut, M.; Belvisi, L.; Bertaglia, A.; Palmioli, A.;
429 Berzi, A.; Trabattoni, D.; Clerici, M.; Fieschi, F.; Bernardi, A. Designing nanomolar
430 antagonists of DC-SIGN-mediated HIV infection: Ligand presentation using molecular
431 rods. *Chem. Commun.* **2015**, *51*, 3816–3819.

432 (31) Luczkowiak, J.; Muñoz, A.; Sánchez-Navarro, M. A.; Ribeiro-viana, R.; Ginieis, A.;
433 Illescas, B. M.; Martín, N.; Delgado, R.; Rojo, J.; Mart, N.; Delgado, R.; Rojo, J.
434 Glycofullerenes inhibit viral infection. *Biomacromolecules* **2013**, *14*, 431–437.

435 (32) Muñoz, A.; Sigwalt, D.; Illescas, B. M.; Luczkowiak, J.; Rodríguez-Pérez, L.; Nierengarten,
436 I.; Holler, M.; Remy, J. S.; Buffet, K.; Vincent, S. P.; Rojo, J.; Delgado, R.; Nierengarten,

437 J. F.; Martín, N. Synthesis of giant globular multivalent glycofullerenes as potent inhibitors
438 in a model of Ebola virus infection. *Nat. Chem.* **2016**, *8*, 50–57.
439 (33) Delbianco, M.; Bharate, P.; Varela-Aramburu, S.; Seeberger, P. H. Carbohydrates in
440 supramolecular chemistry. *Chem. Rev.* **2016**, *116*, 1693–1752.
441 (34) Zhang, Q.; Su, L.; Collins, J.; Chen, G.; Wallis, R.; Mitchell, D. A.; Haddleton, D. M.;
442 Becer, C. R. Dendritic cell lectin-targeting sentinel-like unimolecular glycoconjugates to
443 release an anti-HIV drug. *J. Am. Chem. Soc.* **2014**, *136*, 4325–4332.
444 (35) Morbioli, I.; Porkolab, V.; Magini, A.; Casnati, A.; Fieschi, F.; Sansone, F.
445 Mannosylcalix[n]arenes as multivalent ligands for DC-SIGN. *Carbohydr. Res.* **2017**, *453–*
446 *454*, 36–43.
447 (36) Adak, A. K.; Lin, H. J.; Lin, C. C. Multivalent glycosylated nanoparticles for studying
448 carbohydrate-protein interactions. *Org. Biomol. Chem.* **2014**, *12*, 5563–5573.
449 (37) Martínez-Ávila, O.; Hijazi, K.; Marradi, M.; Clavel, C.; Campion, C.; Kelly, C.; Penadés,
450 S. Gold manno-glyconanoparticles: Multivalent systems to block HIV-1 gp120 binding to
451 the lectin DC-SIGN. *Chem. - Eur. J.* **2009**, *15*, 9874–9888.
452 (38) Ribeiro-Viana, R.; Sánchez-Navarro, M.; Luczkowiak, J.; Koeppe, J. R.; Delgado, R.; Rojo,
453 J.; Davis, B. G. Virus-like glycodendrinanoparticles displaying quasi-equivalent nested
454 polyvalency upon glycoprotein platforms potently block viral infection. *Nat. Commun.*
455 **2012**, *3*, 1303.
456 (39) Hostetler, M. J.; Templeton, A. C.; Murray, R. W. Dynamics of place-exchange reactions
457 on monolayer-protected gold cluster molecules. *Langmuir* **1999**, *15*, 3782–3789.
458 (40) Daniel, M.; Astruc, D. Gold nanoparticles: assembly, supramolecular chemistry, quantum-
459 size-related properties, and applications toward biology, catalysis, and nanotechnology.

460 *Chem. Rev.* **2004**, *104*, 293–346.

461 (41) Love, J. C.; Estroff, L. A.; Kriebel, J. K.; Nuzzo, R. G.; Whitesides, G. M. Self-assembled
462 monolayers of thiolates on metals as a form of nanotechnology. *Chem. Rev.* **2005**, *105*,
463 1103–1170.

464 (42) MacLeod, M. J.; Johnson, J. A. PEGylated N-heterocyclic carbene anchors designed To
465 stabilize gold nanoparticles in biologically relevant media. *J. Am. Chem. Soc.* **2015**, *137*,
466 7974–7977.

467 (43) Remzi Becer, C.; Hoogenboom, R.; Schubert, U. S. Click chemistry beyond metal-catalyzed
468 cycloaddition. *Angew. Chem., Int. Ed.* **2009**, *48*, 4900–4908.

469 (44) Qian, E. A.; Wixtrom, A. I.; Axtell, J. C.; Saebi, A.; Jung, D.; Rehak, P.; Han, Y.; Moully,
470 E. H.; Mosallaei, D.; Chow, S.; Messina, M. S.; Wang, J. Y.; Royappa, A. T.; Rheingold,
471 A. L.; Maynard, H. D.; Král, P.; Spokoyny, A. M. Atomically precise organomimetic cluster
472 nanomolecules assembled via perfluoroaryl-thiol S_NAr chemistry. *Nat. Chem.* **2017**, *9*, 333–
473 340.

474 (45) Messina, M. S.; Axtell, J. C.; Wang, Y.; Chong, P.; Wixtrom, A. I.; Kirlikovali, K. O.;
475 Upton, B. M.; Hunter, B. M.; Shafaat, O. S.; Khan, S. I.; Winkler, J. R.; Gray, H. B.;
476 Alexandrova, A. N.; Maynard, H. D.; Spokoyny, A. M. Visible-light-induced olefin
477 activation using 3D aromatic boron-rich cluster photooxidants. *J. Am. Chem. Soc.* **2016**,
478 *138*, 6952–6955.

479 (46) Floyd, N.; Vijayakrishnan, B.; Koeppe, J. R.; Davis, B. G. Thiyl glycosylate of olefinic
480 proteins: S-linked glycoconjugate synthesis. *Angew. Chem., Int. Ed.* **2009**, *48*, 7798–7802.

481 (47) Pelegri-O'Day, E. M.; Paluck, S. J.; Maynard, H. D. Substituted polyesters by thiol-ene
482 modification: Rapid diversification for therapeutic protein stabilization. *J. Am. Chem. Soc.*

483 **2017**, *139*, 1145–1154.

484 (48) Zhu, S. J.; Ying, H. Z.; Wu, Y.; Qiu, N.; Liu, T.; Yang, B.; Dong, X. W.; Hu, Y. Z. Design,
485 synthesis and biological evaluation of novel podophyllotoxin derivatives bearing 4β-
486 disulfide/trisulfide bond as cytotoxic agents. *RSC Adv.* **2015**, *5*, 103172–103183.

487 (49) Kalhor-Monfared, S.; Jafari, M. R.; Patterson, J. T.; Kitov, P. I.; Dwyer, J. J.; Nuss, J. M.;
488 Derda, R. Rapid biocompatible macrocyclization of peptides with decafluoro-
489 diphenylsulfone. *Chem. Sci.* **2016**, *7*, 3785–3790.

490 (50) Wixtrom, A. I.; Shao, Y.; Jung, D.; Machan, C. W.; Kevork, S. N.; Qian, E. A.; Axtell, J.
491 C.; Khan, S. I.; Kubiak, C. P.; Spokoyny, A. M. Rapid synthesis of redox-active
492 dodecaborane $B_{12}(OR)_{12}$ clusters under ambient conditions. *Inorg. Chem. Front.* **2016**, *3*,
493 711–717.

494 (51) Hill, R. T. Plasmonic biosensors. *Wiley Interdiscip. Rev. Nanomed. Nanobiotechnol.* **2015**,
495 *7*, 152–168.

496 (52) Olaru, A.; Bala, C.; Jaffrezic-Renault, N.; Aboul-Enein, H. Y. Surface plasmon resonance
497 (SPR) biosensors in pharmaceutical analysis. *Crit. Rev. Anal. Chem.* **2015**, *45*, 97–105.

498 (53) Tabarani, G.; Thépaut, M.; Stroebel, D.; Ebei, C.; Vivès, C.; Vachette, P.; Durand, D.;
499 Fieschi, F.; Thepaut, M.; Stroebel, D.; Ebel, C.; Vives, C.; Vachette, P.; Durand, D.; Fieschi,
500 F. DC-SIGN neck domain is a pH-sensor controlling oligomerization. Saxs and
501 hydrodynamic studies of extracellular domain. *J. Biol. Chem.* **2009**, *284*, 21229–21240.

502 (54) Su, S. V; Hong, P.; Baik, S.; Negrete, O. A.; Gurney, K. B.; Lee, B. DC-SIGN binds to
503 HIV-1 glycoprotein 120 in a distinct but overlapping fashion compared with ICAM-2 and
504 ICAM-3. *J. Biol. Chem.* **2004**, *279*, 19122–19132.

505 (55) Menon, S.; Rosenberg, K.; Graham, S. A.; Ward, E. M.; Taylor, M. E.; Drickamer, K.;

506 Leckband, D. E. Binding-site geometry and flexibility in DC-SIGN demonstrated with
507 surface force measurements. *Proc. Natl. Acad. Sci.* **2009**, *106*, 11524–11529.
508 (56) Zhang, Q.; Collins, J.; Anastasaki, A.; Wallis, R.; Mitchell, D. A.; Becer, C. R.; Haddleton,
509 D. M. Sequence-controlled multi-block glycopolymers to inhibit DC-SIGN-gp120 binding.
510 *Angew. Chem., Int. Ed.* **2013**, *52*, 4435–4439.
511 (57) Wang, S.-K.; Liang, P.-H.; Astronomo, R. D.; Hsu, T.-L.; Hsieh, S.-L.; Burton, D. R.;
512 Wong, C.-H. Targeting the carbohydrates on HIV-1: Interaction of oligomannose dendrons
513 with human monoclonal antibody 2G12 and DC-SIGN. *Proc. Natl. Acad. Sci.* **2008**, *105*,
514 3690–3695.
515 (58) Wu, L.; Martin, T. D.; Carrington, M.; KewalRamani, V. N. Raji B cells, misidentified as
516 THP-1 cells, stimulate DC-SIGN-mediated HIV transmission. *Virology* **2004**, *318*, 17–23.
517 (59) Liu, J.; Bartesaghi, A.; Borgnia, M. J.; Sapiro, G.; Subramaniam, S. Molecular architecture
518 of native HIV-1 gp120 trimers. *Nature* **2008**, *455*, 109–113.
519 (60) Mangold, S. L.; Prost, L. R.; Kiessling, L. L. Quinoxalinone inhibitors of the lectin DC-
520 SIGN. *Chem. Sci.* **2012**, *3*, 772–777.
521 (61) Arnáiz, B.; Martínez-Ávila, O.; Falcon-Perez, J. M.; Penadés, S. Cellular uptake of gold
522 nanoparticles bearing HIV gp120 oligomannosides. *Bioconjug. Chem.* **2012**, *23*, 814–825.
523 (62) Boulant, S.; Stanifer, M.; Lozach, P. Y. Dynamics of virus-receptor interactions in virus
524 binding, signaling, and endocytosis. *Viruses* **2015**, *7*, 2794–2815.
525 (63) Řezáčová, P.; Pokorná, J.; Brynda, J.; Kožíšek, M.; Cígler, P.; Lepšík, M.; Fanfrlík, J.;
526 Řezáč, J.; Šašková, K. G.; Sieglová, I.; Plešek, J.; Šícha, V.; Grüner, B.; Oberwinkler, H.;
527 Sedláček', J.; Kräusslich, H. G.; Hobza, P.; Král, V.; Konvalinka, J. Design of HIV protease
528 inhibitors based on inorganic polyhedral metallacarboranes. *J. Med. Chem.* **2009**, *52*, 7132–

529 7141.

530 (64) Lo Conte, M.; Staderini, S.; Chambery, A.; Berthet, N.; Dumy, P.; Renaudet, O.; Marra, A.;
531 Dondoni, A. Glycoside and peptide clustering around the octasilsesquioxane scaffold via
532 photoinduced free-radical thiol-ene coupling. The observation of a striking glycoside cluster
533 effect. *Org. Biomol. Chem.* **2012**, *10*, 3269–3277.

534 (65) Levine, D. J.; Stöhr, J.; Falese, L. E.; Ollesch, J.; Wille, H.; Prusiner, S. B.; Long, J. R.
535 Mechanism of scrapie prion precipitation with phosphotungstate anions. *ACS Chem. Biol.*
536 **2015**, *10*, 1269–1277.

537 (66) Pöhlmann, S.; Baribaud, F.; Lee, B.; Leslie, G. J.; Sanchez, M. D.; Hiebenthal-Millow, K.;
538 Münch, J.; Kirchhoff, F.; Doms, R. W. DC-SIGN interactions with human
539 immunodeficiency virus type 1 and 2 and simian immunodeficiency virus. *J. Virol.* **2001**,
540 *75*, 4664–4672.

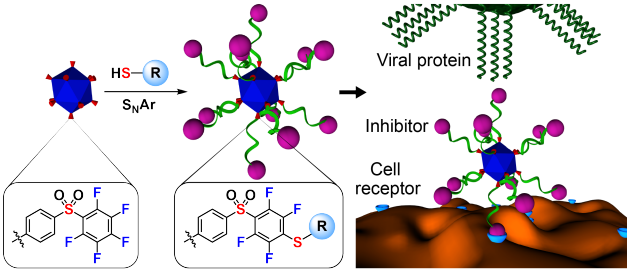

For Table of Contents Only